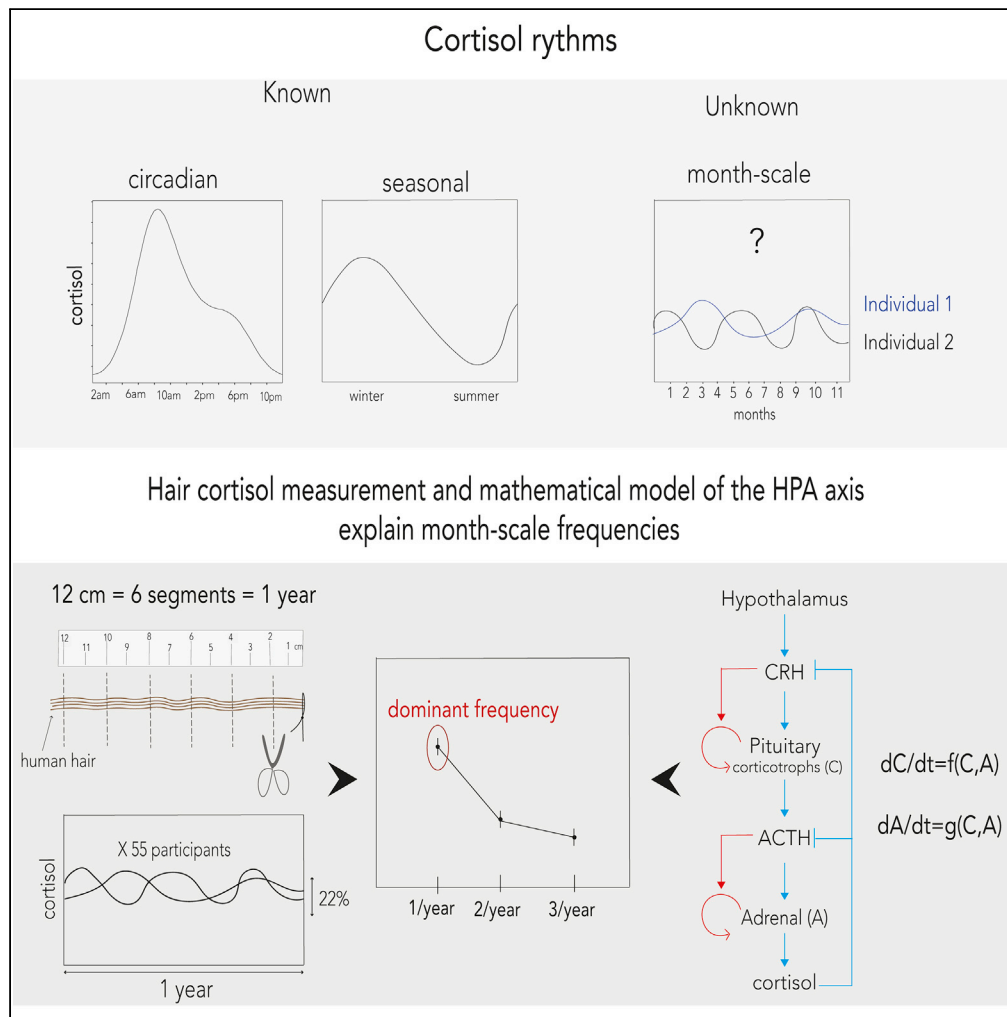


Article

Timescales of Human Hair Cortisol Dynamics



Lior Maimon, Tomer Milo, Rina S. Moyal, Avi Mayo, Tamar Danon, Anat Bren, Uri Alon

uri.alon@weizmann.ac.il

HIGHLIGHTS
Longitudinal cortisol over a year was measured using hair from 55 healthy individuals

A method was developed to adjust for decline along the length of the hair

Cortisol showed non-seasonal fluctuations with periods of months to a year

These fluctuations can be explained by turnover time of cortisol-related glands



Article

Timescales of Human Hair Cortisol Dynamics

Lior Maimon,^{1,2} Tomer Milo,^{1,2} Rina S. Moyal,¹ Avi Mayo,¹ Tamar Danon,¹ Anat Bren,¹ and Uri Alon^{1,3,*}

SUMMARY

Cortisol is a major human stress hormone, secreted within minutes of acute stress. Cortisol also has slower patterns of variation: a strong circadian rhythm and a seasonal rhythm. However, longitudinal cortisol dynamics in healthy individuals over timescales of months has rarely been studied. Here, we measured longitudinal cortisol in 55 healthy participants using 12 cm of hair, which provides a retrospective measurement over one year. Individuals showed (non-seasonal) fluctuations averaging about 22% around their baseline. Fourier analysis reveals dominant slow frequencies with periods of months to a year. These frequencies can be explained by a mathematical model of the hormonal cascade that controls cortisol, the HPA axis, when including the slow timescales of tissue turnover of the glands. Measuring these dynamics is important for understanding disorders in which cortisol secretion is impaired over months, such as mood disorders, and to test models of cortisol feedback control.

INTRODUCTION

Cortisol is a major stress hormone in humans. It is secreted in response to psychological and physiological stress, under control of a cascade of hormones called the HPA (hypothalamus-pituitary-adrenal) axis. Cortisol has receptors in most cell types and exerts widespread actions that help the organism to prepare for stressors and to cope with them (Buckingham, 2009; McEwen, 1998; Sapolsky et al., 2000). Cortisol dysregulation is implicated in physiological and psychological pathologies, such as mood disorders, including depression (Daban et al., 2005; Ehler et al., 2001; Nemeroff et al., 1992; Pearson Murphy, 1991; Sriram et al., 2012; Watson and Mackin, 2006; Wingenfeld and Wolf, 2015).

Cortisol has dynamics on several timescales (Figure 1A). It shows ultradian pulses throughout the day that last about 60–90 min (Young et al., 2004). Pulse amplitude is largest in the morning, forming a sizable circadian pattern (Walker et al., 2010). Cortisol also has a seasonal rhythm, which peaks in late winter (Hadlow et al., 2018; Miller et al., 2016; Tendler et al., 2020). The amplitude of this seasonal rhythm is a few percent in temperate climes and rises to tens of percents at high latitudes. Detecting this seasonal rhythm requires averaging over many individuals. On the timescale of decades, cortisol generally decreases at old age on average (Sharma et al., 1989).

Overlaid on top of these daily and seasonal patterns is the response of cortisol to the stressors that occur over time. Thus, one expects cortisol dynamics to fluctuate over weeks, months, and years in each individual. However, the nature of these slow fluctuations and their typical timescale have not been quantified.

Understanding fluctuations on a timescale of months is important to better understand the feedback loops in the HPA axis. Cortisol inhibits its upstream hormones (Figure 1B) in a classic feedback loop that acts on the timescale of minutes to hours (Andersen et al., 2013; Ronald De Kloet et al., 1998). This feedback can explain ultradian rhythms on the scale of hours (Walker et al., 2010). A recent model by Karin et al., 2020 points to an additional feedback loop, which acts over months. In this feedback loop, the functional mass of the glands in the HPA axis changes over time, under the control of the hormones that act as growth factors (Bicknell et al., 2001; Gertz et al., 1987; Horvath et al., 1999; Kataoka et al., 1996; Nolan et al., 1998; Westlund et al., 1985) (Figure 1C). This effectively forms a feedback loop between two glands in the HPA axis, the adrenal cortex cells and the pituitary corticotrophs (Figure 1D). This feedback loop is predicted to have a typical timescale of about a year, due to the slow timescale of tissue turnover (Figure 1E). Intuitively, this model predicts that stressors over time would stimulate the natural period of this feedback loop,

¹Department Molecular Cell Biology, Weizmann Institute of Science, Rehovot 76100, Israel

²These authors contributed equally

³Lead Contact

*Correspondence: uri.alon@weizmann.ac.il
<https://doi.org/10.1016/j.isci.2020.101501>



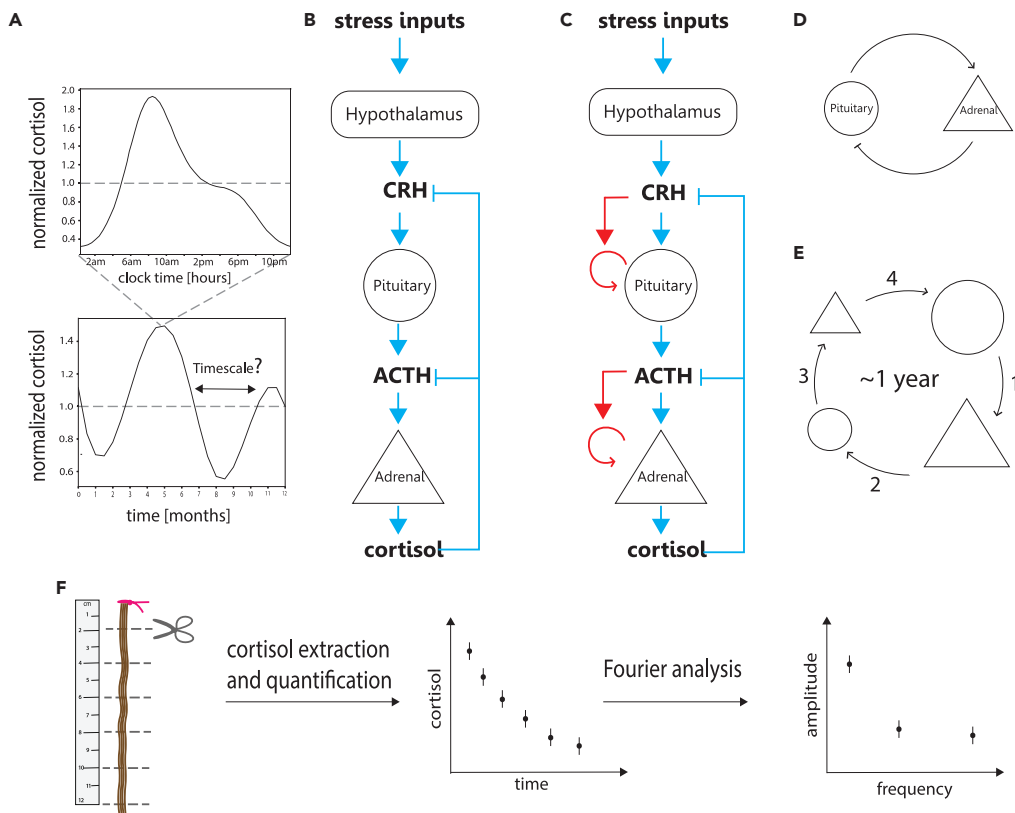


Figure 1. Cortisol Secretion Is Governed by the HPA Axis

(A) Top panel: cortisol shows circadian changes over the day, adapted from [Chan and Debono, \(2010\)](#). Bottom panel: varying stress inputs can cause fluctuations over months, whose timescale is the subject of this study.

(B) Classic model of the HPA axis in which stress inputs cause corticotropin-releasing hormone (CRH) secretion from the hypothalamus, causing the pituitary corticotrophs to secrete adrenocorticotrophic hormone (ACTH), which in turn causes cells in the adrenal cortex to secrete cortisol. Cortisol inhibits the secretion of the upstream hormones.

(C) The Karin et al. model, which includes the effect of hormones on gland proliferation (red arrows), which introduces the slow timescale of tissue turnover (weeks-months).

(D) The adrenal cortex and pituitary corticotrophs effectively form a negative feedback loop when considering the slow timescale of months.

(E) An increase in pituitary corticotroph cells' total mass leads to increased ACTH secretion, which increases adrenal cortex mass (1). This leads to an increase in cortisol, which inhibits ACTH, causing a reduction in corticotroph cells (2). This feedback loop with cell turnover times of few weeks has a resonance frequency with an overall timescale of a year.

(F) Schematic overview of this study: longitudinal hair cortisol over 1 year is analyzed using Fourier transform to detect frequencies of fluctuations.

leading to noisy fluctuations of cortisol with a timescale of about a year (added on top of the much smaller seasonal pattern).

Understanding cortisol fluctuations in healthy individuals can also set a baseline to compare with the situation in mood disorders that play out over months, such as depression and bipolar disorder ([Belvederi et al., 2016](#)). Future studies of cortisol dynamics in individuals with mood disorders would benefit from a solid understanding of the control group, namely, cortisol fluctuations in healthy individuals.

Here we explore the dynamics of cortisol in healthy participants using longitudinal measurements over 1 year. We use hair cortisol, a measure that allows retrospective quantification ([D'Anna-Hernandez et al., 2011](#); [Davenport et al., 2006](#); [Mayer et al., 2019](#)). Cortisol passively lies in hair. Each centimeter of hair corresponds to about 1 month of growth, and thus analyzing hair allows measurement of cortisol levels averaged over long times ([D'Anna-Hernandez et al., 2011](#); [Smy et al., 2016](#)). We developed a procedure to adjust for the decay of cortisol over 12-cm hair samples and use Fourier analysis to quantify the contribution

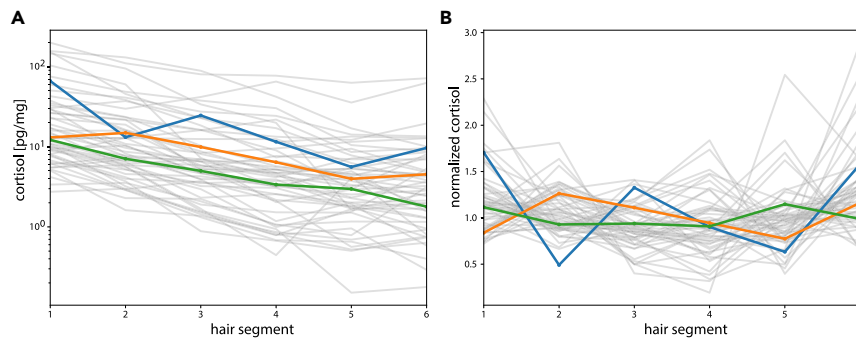


Figure 2. Longitudinal Cortisol Measurements from Human Hair

(A) Cortisol time series from 55 participants. Each time series has 6 points corresponding to six 2-cm segments of hair, representing about 1 year of growth.
(B) Normalized cortisol for the same participants, after correction for decline along the hair. Highlighted in color are three examples of individual cortisol time series.

of different frequencies in the signal. We find fluctuations with a standard deviation of about 22% around each individual's baseline and a dominant, non-seasonal frequency component of 1 year. We show that the gland-mass feedback loop model can explain these frequencies.

RESULTS

Longitudinal Cortisol Fluctuates around Its Baseline

We collected 12 cm of hair from healthy participants and assayed cortisol using ELISA in 2-cm segments. This provided a longitudinal time-series of six time points over about a year of growth (Figure 2A).

We corrected each time series for the decline of cortisol in distal segments by fitting an exponential decay model to each participant's cortisol measurements (see Methods). The mean decay coefficient was $\bar{\alpha} = 2.2 \pm 0.2$ [year^{-1}] (standard error of the mean, SEM). The exponential fit allowed estimate of the baseline cortisol for each individual. The baseline varied about 30-fold between individuals, as can be seen in Figure 2A.

After normalizing by the decline, the fluctuations around each individual baseline can be seen in Figure 2B.

Normalized cortisol showed fluctuations around the mean with an average coefficient of variance (CV) of 28%. When accounting for experimental noise with $\text{CV} = 14\%$ (see Methods), one obtains fluctuations with $\text{CV} = 24\%$.

Longitudinal Hair Cortisol Shows a Dominant 1 Year⁻¹ Frequency Component

To explore the frequencies underlying these fluctuations, we used Fourier analysis, which quantifies the contributions of different frequencies to the signal. Six segments allow three frequencies to be detected: 1 [year^{-1}], 2 [year^{-1}], and 3 [year^{-1}], representing periods of a year, 6 months, and 4 months, respectively.

We averaged the Fourier amplitudes over the participants. The highest mean amplitude was obtained at the slowest frequency, 1 [year^{-1}] (Figure 3, black dots). This amplitude was about 1.45 ± 0.17 times higher than the amplitude at the highest frequency, 3 [year^{-1}].

To test the statistical significance of this observation, we compared the Fourier spectrum to a null model constructed by shuffled data and subjected to the same correction for cortisol decline (Methods, Figure 3, gray dots). The amplitude of the 1 [year^{-1}] frequency was significantly higher than shuffled control with a large effect size ($p = 0.004$, Cohens $d = 3.8$, non-parametric $p = 0.002$, Cliff's delta = 0.99).

Note that the null model has lower amplitudes in the 1 [year^{-1}] frequency compared with the other frequencies. This decrease in the slowest frequency is due to correction for the cortisol decline along the hair: the subtraction (in log-transformed variables) of an exponential fit from the raw signals removes a major portion of the slowest frequency component from the normalized signals. This is generally true also for

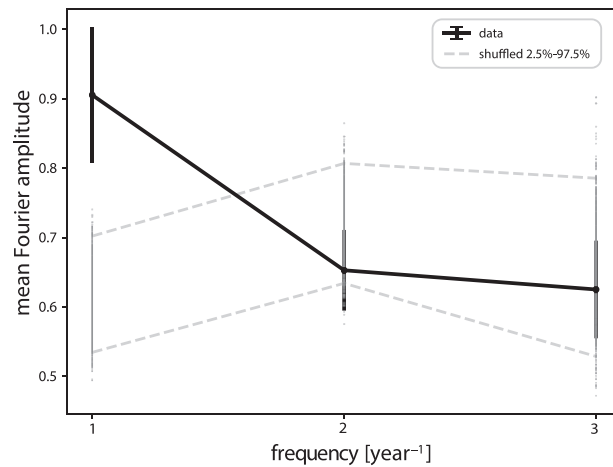


Figure 3. Hair Cortisol Shows Fluctuations with a Dominant Period of 1 Year

Fourier amplitudes averaged over participants quantify the contribution of each frequency component (1[year⁻¹], 2[year⁻¹], and 3[year⁻¹]) to the cortisol signal (black dots). Error bars (SEM) were calculated by bootstrapping the participants. Shuffled control is shown as gray dots (1,000 repeats), with 97.5% and 2.5% confidence intervals shown in dashed gray lines. The amplitude of the 1 [year⁻¹] frequency is significantly higher than shuffled control, $p = 0.004$.

random data, such as those generated from a normal distribution. The experimental data show high amplitude at low frequency (1 [year⁻¹]) despite this effect.

We also conducted a non-parametric correction for cortisol decline (see [Methods Supplemental Information](#), section S4), which gave the same conclusion of a dominant 1 [year⁻¹] frequency component in cortisol spectrum.

We also corrected for seasonality—the effect of the month of the year on cortisol—by fitting the decline-corrected cortisol to a cosinor model. Cortisol showed a seasonality effect of about 15%. When corrected for seasonality ([Supplemental Information](#), section S3), the CV of the decline-corrected fluctuations dropped from 24% to 22%. The year⁻¹ frequency remains the dominant frequency. This indicates that the slow cortisol variations in each individual go beyond a seasonal effect.

Model of the HPA Axis with Gland Mass Dynamics can Explain the Year-scale Fluctuations

We asked what biological processes might underlie the observed frequency spectrum of hair cortisol, with large amplitude at year⁻¹ frequency. One possibility is that stressor inputs to the HPA axis have dominant low-frequency components. For example, due to life events, some periods of several months may be more stressful than others ([Dettenborn et al., 2010](#); [Rothman, 1972](#); [Staufenbiel et al., 2013](#)), contributing to the observed fluctuations (beyond the variation with season).

Here we consider in detail an alternative explanation, in which the interactions within the HPA axis contribute to the low-frequency cortisol fluctuations. We thus ask whether stressor inputs randomly distributed over time can generate cortisol fluctuations with typical fluctuations of a year.

We simulated and compared two models of the HPA axis. First is the classic HPA model ([Figure 1B](#)), in which the only feedback mechanism is inhibition by cortisol to upstream hormones. This model has timescales given by the hormone half-lives, namely, hours. Simulating this model with white-noise stress input results in a Fourier spectrum without dominant year⁻¹ frequency. Instead, all frequencies are found with approximately the same amplitude. Applying the decline correction to the simulated data, as done to the experimental data, results in a spectrum that is indistinguishable from the null model ([Figure 4A](#)).

In contrast, we simulated the model of Karin et al. ([Figure 1C](#)), which includes the changes of gland masses with typical timescale of months. Using the same input signals, this model provides a dominant 1[year⁻¹] frequency component ([Figure 4B](#)). The period of 1 year arises from the tissue turnover times, which are

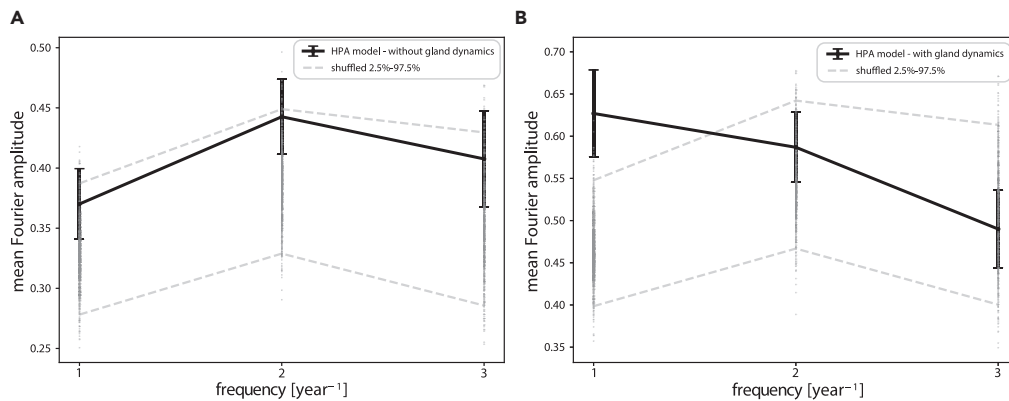


Figure 4. HPA Model with Gland Mass Dynamics Is Sufficient to Explain the Year-Scale Fluctuations in Cortisol
(A) Textbook HPA model includes a cascade of hormones with negative feedback of cortisol on its upstream hormones (Figure 1B). The Fourier spectrum in response to white noise input is similar to the null model.
(B) Karin et al. model with gland mass dynamics (Figure 1C) shows a Fourier spectrum with a dominant [year⁻¹] frequency component. The black dots are the mean Fourier amplitude with SEM error bars. Dashed lines: 2.5% and 97.5% confidence intervals of a shuffled data control. Both simulations and null models were subjected to the decline correction.

on the order of a few weeks, due to the 2π term in the equation period = $2\pi/\text{frequency}$. The only model parameters that affect the timescales of months-years are the two tissue turnover times. All other model parameters are of the fast timescale of hours, such as hormone turnover times and secretion rates, and do not contribute to the dynamics on this slow timescale. This can be shown analytically using the Laplace transform on linearized model equations (Supplemental Information, section S6), as well as by a detailed sensitivity analysis using simulations (Supplemental Information, section S5).

We find that the turnover times of the two tissues in the model, corticotrophs and cortisol-secreting cells in the adrenal cortex, can range from days to months to obtain a similar shape to the observed Fourier spectrum. Thus, we conclude that the model is sufficient to explain the timescales of the measured cortisol fluctuations.

DISCUSSION

We analyzed longitudinal hair cortisol in healthy participants. Cortisol fluctuated by about 22% around the baseline, with variations that have a dominant low-frequency component with a period of 1 year. This variation goes beyond the effect of seasonality. The slow variations are consistent with a recent model of the HPA axis, which can explain low frequencies by the hormonal regulation of the functional mass of the cells that secrete adrenocorticotrophic hormone and cortisol, namely, pituitary corticotroph cells and adrenal cortex cells. The timescale of months to years arises due to the slow turnover time of the tissues.

Hair has advantages for longitudinal cortisol profiling on the timescale of months, due to its low invasiveness, ease of acquisition, convenient storage, and the ability of hair to record cortisol from the past. A technical advance in this study was to correct for the decay in cortisol distally along the hair. This decay was reported in several previous studies and has led many researchers to use only the first few centimeters of hair closest to the scalp (Kirschbaum et al., 2009; Mayer et al., 2019; Schonblum et al., 2018). Here we corrected the decline by fitting an exponential decay to each time series and compared this to shuffled controls. This allowed us to estimate the extent and significance of the Fourier amplitudes over a year of dynamics.

One limitation of this study is that 12 cm of hair does not allow rhythms slower than 1 year to be detected. Indeed, the HPA model suggests that such slower rhythms are expected. As cortisol in most samples decayed close to background detection levels after 12 cm, a future longitudinal study with multiple hair samples is needed to estimate the amplitude of slower Fourier frequencies.

The present agreement with the Karin et al. HPA model adds to a picture in which the functional masses of the cells in the HPA axis are important variables. These masses are not considered in standard models of

the HPA axis. Karin et al. showed that such mass changes are sufficient to explain HPA dysregulation after prolonged stress. (Tendler et al., 2020) proposed that the same model can explain seasonal entrainment of hormones and their seasonal peaks and troughs. Here, we propose that the mass changes provide a “memory” to the HPA axis, which can integrate over the fast timescale fluctuations of stress inputs to generate fluctuations that last on the timescale of a year. Future work can further test this model by measuring gland masses over time and correlating them with hormonal measurements.

The HPA model studied here is not the only possible explanation for the slow fluctuations with periods of months to years. These fluctuations may also arise due to slow timescales in the distribution of stressors over time. Such slow timescales arise in many human activity patterns, which have long-tailed distributions of intervals between events (Vázquez et al., 2006). Investigating the role of the temporal stressor distribution requires following stressors over time and may be the focus of future work. Additional effects can introduce long timescales, including the effects of epigenetic regulation in the HPA axis.

The present study can serve as a baseline for future exploration of stress-related pathologies. For example, mood disorders display HPA dysregulation, but the precise dynamics of this dysregulation remains to be clarified in conditions such as bipolar disorder. Hair offers a rare opportunity to look retrospectively from the time of first diagnosis, showing the dynamical prodrome to disease onset. Cortisol dynamics can be used to test models of pathology, and to provide a detailed diagnostic for HPA axis function.

In the long term, one may envision using hair cortisol longitudinal dynamics as a basis for stabilizers of psychological diseases that involve dysregulation of the HPA axis on the scale of months (other HPA syndromes such as Addisonian crisis can have much faster timescales and cannot rely on hair measurements). In this paradigm, the goal is to return dysregulated HPA function back to baseline using a feedback-control approach. One measures cortisol, simulates a model of the axis, and determines the optimal dose of HPA agonists or antagonists to take in the next time period (e.g., a month) to return dysregulated HPA function back to baseline (Ben-Zvi et al., 2009). Following the interventions, hair measurements can be used to test if the desired state was reached.

Limitations of the Study

This study involved a sample of only 55 individuals from one country. Future work can enlarge sample size and sample additional populations, which is important given the large person-to-person variability in cortisol. Use of other methods to measure cortisol, such as mass spectrometry, can test the validity of the results. Use of multiple short hair samples from the same individual can extend the study period beyond 12 months and test the validity of the decline correction.

Resource Availability

Lead Contact

Further information and requests for resources should be directed to and will be fulfilled by the Lead Contact, Uri Alon (uri.alon@weizmann.ac.il).

Materials Availability

This study did not generate new unique reagents.

Data and Code Availability

The data and code generated during this study are available at <https://github.com/tomermilo/hair-cortisol>.

METHODS

All methods can be found in the accompanying [Transparent Methods supplemental file](#).

SUPPLEMENTAL INFORMATION

Supplemental Information can be found online at <https://doi.org/10.1016/j.isci.2020.101501>.

ACKNOWLEDGMENTS

We thank Alon Bar, Melvin McInnis, Holli Bertram, Omer Karin, Avichai Tendler, Ron Rotkopf, Michal Sharon, and David Glass for discussions. U.A. is the incumbent of the Abisch-Frenkel professorial chair. This project has received funding from the European Research Council (ERC) under the European Union's Horizon 2020 Research and Innovation Program (grant agreement No 856487).

AUTHOR CONTRIBUTIONS

L.M., T.M., and U.A. designed the study, L.M. recruited participants, L.M., R.S.M., T.D. and A.B performed the experiments, T.M., A.M. and L.M. analyzed the data, L.M., T.M. and U.A. wrote the paper.

DECLARATION OF INTERESTS

The authors declare no competing interests.

Received: May 14, 2020

Revised: July 23, 2020

Accepted: August 21, 2020

Published: September 25, 2020

REFERENCES

- Andersen, M., Vinther, F., and Ottesen, J.T. (2013). Mathematical modeling of the hypothalamic-pituitary-adrenal (HPA) axis, including hippocampal mechanisms. *Math. Biosci.* 246, 122–138.
- Belvederi, M., Prestia, D., Mondelli, V., Pariante, C., Patti, S., Olivieri, B., Arzani, C., Masotti, M., Respino, M., Antonioli, M., et al. (2016). The HPA axis in bipolar disorder : systematic review and meta-analysis. *Psychoneuroendocrinology* 63, 327–342.
- Ben-Zvi, A., Vernon, S.D., and Broderick, G. (2009). Model-based therapeutic correction of hypothalamic-pituitary-adrenal axis dysfunction. *PLoS Comput. Biol.* 5, e1000273.
- Bicknell, A.B., Lomthaisong, K., Woods, R.J., Hutchinson, E.G., Bennett, H.P.J., Gladwell, R.T., and Lowry, P.J. (2001). Characterization of a serine protease that cleaves pro- γ -melanotropin at the adrenal to stimulate growth. *Cell* 105, 903–912.
- Buckingham, J.C. (2009). Glucocorticoids: exemplars of multi-tasking. *Br. J. Pharmacol.* 147, S258–S268.
- Chan, S., and Debono, M. (2010). Review: replication of cortisol circadian rhythm: new advances in hydrocortisone replacement therapy. *Ther. Adv. Endocrinol. Metab.* 1, 129–138.
- D'Anna-Hernandez, K.L., Ross, R.G., Natvig, C.L., and Laudenslager, M.L. (2011). Hair cortisol levels as a retrospective marker of hypothalamic-pituitary axis activity throughout pregnancy: comparison to salivary cortisol. *Physiol. Behav.* 104, 348–353.
- Daban, C., Vieta, E., Mackin, P., and Young, A.H. (2005). Hypothalamic-pituitary-adrenal axis and bipolar disorder. *Psychiat. Clin. North Am.* 28, 469–480.
- Davenport, M.D., Tiefenbacher, S., Lutz, C.K., Novak, M.A., and Meyer, J.S. (2006). Analysis of endogenous cortisol concentrations in the hair of rhesus macaques. *Gen. Comp. Endocrinol.* 147, 255–261.
- Dettenborn, L., Tietze, A., Bruckner, F., and Kirschbaum, C. (2010). Higher cortisol content in hair among long-term unemployed individuals compared to controls. *Psychoneuroendocrinology* 35, 1404–1409.
- Ehler, U., Gaab, J., and Heinrichs, M. (2001). Psychoneuroendocrinological contributions to the etiology of depression, posttraumatic stress disorder, and stress-related bodily disorders: the role of the hypothalamus-pituitary-adrenal axis. *Biol. Psychol.* 57, 141–152.
- Gertz, B.J., Contreras, L.N., McComb, D.J., Kovacs, K., Tyrrell, J.B., and Dallman, M.F. (1987). Chronic administration of corticotropin-releasing factor increases pituitary corticotroph number. *Endocrinology* 120, 381–388.
- Hadlow, N., Brown, S., Wardrop, R., Conradie, J., and Henley, D. (2018). Where in the world? Latitude, longitude and season contribute to the complex co-ordinates determining cortisol levels. *Clin. Endocrinol.* 89, 299–307.
- Horvath, E., Kovacs, K., and Scheithauer, B. (1999). Pituitary hyperplasia. *Pituitary* 1, 169–179.
- Karin, O., Raz, M., Tendler, A., Bar, A., Kohanim, Y.K., Milo, T., and Alon, U. (2020). Hormonal dysregulation after prolonged HPA axis activation can be explained by changes of adrenal and corticotroph masses. *bioRxiv*. <https://doi.org/10.1101/2020.01.01.892596>.
- Kataoka, Y., Ikehara, Y., and Hattori, T. (1996). Cell proliferation and renewal of mouse adrenal cortex. *J. Anat.* 188 (Pt 2), 375–381. <http://www.ncbi.nlm.nih.gov/pubmed/8621337>.
- Kirschbaum, C., Tietze, A., Skoluda, N., and Dettenborn, L. (2009). Hair as a retrospective calendar of cortisol production-Increased cortisol incorporation into hair in the third trimester of pregnancy. *Psychoneuroendocrinology* 34, 32–37.
- Mayer, S.E., Abelson, J.L., Briggs, H., Skaza, J., Kirschbaum, C., and Stalder, T. (2019). How does hair cortisol assessment correspond to saliva measures and to lab-based probes of HPA axis regulatory function? *Psychoneuroendocrinology* 107, 50–51.
- McEwen, B.S. (1998). Protective and damaging effects of stress mediators. *N. Engl. J. Med.* 338, 171–179.
- Miller, R., Stalder, T., Jarczok, M., Almeida, D.M., Badrick, E., Bartels, M., Boomsma, D.I., Coe, C.L., Dekker, M.C.J., Donzella, B., et al. (2016). The CIRCORT database: reference ranges and seasonal changes in diurnal salivary cortisol derived from a meta-dataset comprised of 15 field studies. *Psychoneuroendocrinology* 73, 16–23.
- Nemeroff, C.B., Krishnan, K.R.R., Reed, D., Leder, R., Beam, C., and Dunnick, N.R. (1992). Adrenal gland enlargement in major depression: a computed tomographic study. *Arch. Gen. Psychiatry* 49, 384–387.
- Nolan, L.A., Kavanagh, E., Lightman, S.L., and Levy, A. (1998). Anterior pituitary cell population control: basal cell turnover and the effects of adrenalectomy and dexamethasone treatment. *J. Neuroendocrinol.* 10, 207–215.
- Pearson Murphy, B.E. (1991). Steroids and depression. *J. Steroid Biochem. Mol. Biol.* 38, 537–559.
- Ronald De Kloet, E., Vreugdenhil, E., Joels, M., De Kloet, E.R., Oitzl, M.S., Joëls, M., and Joëls, J. (1998). Brain Corticosteroid Receptor Balance in Health and Disease*, 19 (Endocrine reviews), pp. 269–301.
- Rothman, A.I. (1972). Longitudinal study of medical students. *Acad. Med.* 47, 901–902.
- Sapolsky, R.M., Romero, L.M., and Munck, A.U. (2000). How do glucocorticoids influence stress responses? Integrating permissive, suppressive, stimulatory, and preparative actions*. *Endocr. Rev.* 21, 55–89.

Schonblum, A., Arnon, L., Ravid, E., Salzer, L., Hadar, E., Meizner, I., Wiznitzer, A., Weller, A., and Koren, L. (2018). Can hair steroids predict pregnancy longevity? *Reprod. Biol.* *18*, 410–415.

Sharma, M., Palacios-Bois, J., Schwartz, G., Iskandar, H., Thakur, M., Quirion, R., and Nair, N.P.V. (1989). Circadian rhythms of melatonin and cortisol in aging. *Biol. Psychiatry* *25*, 305–319.

Smy, L., Shaw, K., Amstutz, U., Smith, A., Berger, H., Carleton, B., and Koren, G. (2016). Hair cortisol as a hypothalamic-pituitary-adrenal axis biomarker in pregnant women with asthma: a retrospective observational study. *BMC Pregnancy Childbirth* *16*, 176.

Sriram, K., Rodriguez-Fernandez, M., and Doyle, F.J. (2012). Modeling cortisol dynamics in the neuro-endocrine axis distinguishes normal, depression, and post-traumatic stress disorder (PTSD) in humans. *PLoS Comput. Biol.* *8*, e1002379.

Staufenbiel, S.M., Penninx, B.W.J.H., Spijker, A.T., Elzinga, B.M., and van Rossum, E.F.C. (2013). Hair cortisol, stress exposure, and mental health in humans: a systematic review. *Psychoneuroendocrinology* *38*, 1220–1235.

Tendler, A., Bar, A., Mendelsohn-Cohen, N., Karin, O., Korem, Y., Maimon, L., Milo, T., Raz, M., Mayo, A., Tanay, A., and Alon, U. (2020). Human hormone seasonality. *bioRxiv*. <https://doi.org/10.1101/2020.02.13.947366>.

Vázquez, A., Oliveira, J.G., Dezsö, Z., Goh, K. II, Kondor, I., and Barabási, A.L. (2006). Modeling bursts and heavy tails in human dynamics. *Phys. Rev. E - Stat. Nonlin. Soft Matter Phys.* *73*, 036127.

Walker, J.J., Terry, J.R., and Lightman, S.L. (2010). Origin of ultradian pulsatility in the hypothalamic-pituitary-adrenal axis. *Proc. Biol. Sci.* *277*, 1627–1633.

Watson, S., and Mackin, P. (2006). HPA axis function in mood disorders. *Psychiatry* *5*, 166–170.

Westlund, K.N., Aguilera, G., and Childs, G.V. (1985). Quantification of morphological changes in pituitary corticotropes produced by *in vivo* corticotropin-releasing factor stimulation and adrenalectomy*. *Endocrinology* *116*, 439–445.

Wingenfeld, K., and Wolf, O.T. (2015). Effects of cortisol on cognition in major depressive disorder, posttraumatic stress disorder and borderline personality disorder - 2014 Curt Richter Award Winner. *Psychoneuroendocrinology* *51*, 282–295.

Young, E.A., Abelson, J., and Lightman, S.L. (2004). Cortisol pulsatility and its role in stress regulation and health. *Front. Neuroendocrinol.* *25*, 69–76.

iScience, Volume 23

Supplemental Information

Timescales of Human

Hair Cortisol Dynamics

Lior Maimon, Tomer Milo, Rina S. Moyal, Avi Mayo, Tamar Danon, Anat Bren, and Uri Alon

1 Supplemental Information for “Timescales of human hair cortisol 2 dynamics over one year”

3 Transparent Methods

4 *Ethics statement*

5 The study protocol was approved by the Review Board of the Weizmann Institute of
6 Science (study code: 706-1). Written informed consent was obtained from all participants.

7 *Participants*

8 Healthy participants (N=59, females=45, average age=27±6) were recruited during
9 January-December of 2019 through social media. Inclusion criteria: participants older
10 than 18 years, with at least 12 centimeters of natural hair with no cosmetic treatment such
11 as dying or perming (Cooper, 2015). Exclusion criteria: diagnosis of a mental,
12 psychological or endocrine disorder, consumption of steroids, psychiatric drugs or other
13 drugs that might affect the endocrine system during the year prior to participation, and
14 pregnancy in the year before participating. Oral contraceptives were allowed as long as
15 there was no change in prescription during the year prior to participation. Each subject
16 was asked to complete a personal information questionnaire prior to the collection of a
17 hair sample. The study was anonymous; each hair sample received a serial number. Male
18 height was 179±6 cm, weight 73±11 kg and BMI (body mass index) 22±3; Female height
19 was 164±6 cm, weight 61±9 kg and BMI 23±3 (all values are mean±STD). 26% of the
20 females reported taking oral contraceptives.

21 *Hair Cortisol Measurements*

22 A lock of hair (a pencil-width group of about 100 hair strands) from the vertex posterior
23 area (Cooper, 2015; Sauv e et al., 2007) of the head was tied with a thread and cut with
24 fine scissors as close to the scalp as possible. We estimate that hair is cut at 0.8±0.1 cm
25 from the scalp, in agreement with Cooper et al. (2015). Cut samples were masking-taped
26 at their distal end to a piece of aluminum foil; the tied thread marked the proximal end.
27 Samples were kept in the laboratory at room temperature before analysis.

28 We adapted a protocol by Schonblum et al. (2018) for the extraction and measurement
29 of hair cortisol. The first 12 centimeters of each hair sample, starting from the proximal
30 end, were segmented to six 2 cm segments (segments of 1 cm dropped below the
31 detection threshold too often and thus 2 cm segments were used). The segments were
32 placed in vials (Fisherbrand, 21x70 mm) and washed twice with 5 ml isopropanol while

33 mixing on an orbital rotator for 3 minutes. Isopropanol was then decanted and the open
34 vials were left in a chemical hood to dry overnight. Then, 2 ml of methanol was added to
35 each vial, sonicated for 60 min, and incubated overnight (approximately 20 hours) at 50°C
36 while shaking. The following day, all the methanol was transferred to 2 ml Eppendorf
37 tubes and centrifuged for 10 minutes at 4°C. Methanol (1.5 ml) from each tube was
38 transferred to a glass vial (Falcon, 12x75 mm) and evaporated under a stream of nitrogen
39 at 45 °C. Samples were reconstituted in 10% methanol and 90% assay buffer provided
40 by the kit manufacturer and cortisol was quantified using competitive Enzyme-Linked
41 Immunosorbent Assays (ELISA; Salimetrics Europe, Newmarket, cat.no1-3002-5 for
42 cortisol, UK). Reported antibody cross-reactivity was 19.2% with dexamethasone, and
43 less than 1% with 15 other tested steroids. Linearity was observed between 30-70 mg of
44 hair, hence we used 30-70 mg of hair to measure cortisol. The assay detection threshold
45 was 112 pg as specified by the manufacturer. All 6 segments from the 12 cm sample of
46 hair from each participant were analyzed in the same batch of washing, sonication,
47 extraction and ELISA plate. To control for inter-assay variation, we generated a standard
48 curve for each plate, consisting of 6 known concentrations of cortisol supplied by the kit
49 manufacturer assayed in 6 wells. To estimate the inter-batch variation, we assayed
50 multiple standard hair samples. Each standard sample was taken from a large, well-
51 mixed, sample of hair collected from a single individual. The coefficient of variation
52 (CV=STD/mean) of 13 standard samples measured on 2 different day was 14%.

53 We included in this study the 55 participants (32 females) with all 6 cortisol measurements
54 above detection threshold. Mean cortisol levels did not show a significant correlation with
55 age (spearman $r=0.19$, $p=0.2$), weight (spearman $r=0.01$, $p=0.9$), height (spearman
56 $r=0.06$, $p=0.7$), and BMI (spearman $r=0.03$, $p=0.8$). Mean cortisol levels did not
57 significantly differ between the sex groups (Mann Whitney U test, $p=0.22$) or by taking
58 oral contraceptives (Mann Whitney U test, $p=0.35$).

59 *Analysis of cortisol time series*

60 Each hair sample provided six 2 cm segments. The average rate of scalp hair growth in
61 humans is approximately 1 cm/month, with a reported range of 0.6 to 1.5 cm a month
62 (Cooper, 2015); we thus assumed that each 2 cm segment represents two months of
63 growth and contains cortisol that accumulated during that period. Due to factors including
64 hair washing (Hamel et al., 2011), cortisol levels in hair decline as a function of distance
65 from the scalp (Gao et al., 2010; Kirschbaum et al., 2009; Steudte et al., 2011). Studies
66 on glycosylated proteins in hair showed a similar decline that was well-described as
67 exponential with time (Nissimov et al., 2007). To account for the decline, we performed a
68 linear regression on the log of the measurements, equivalent to assuming an exponential
69 decline of $A_j \exp(-\alpha_j t_i)$ for individual j , where t_i is the time corresponding to segment $i =$
70 $1..6$, assuming hair growth rate of 1 *cm/month*. We constrained the slope to be negative

71 ($\alpha_j > 0$). Thus, if \hat{c}_{ij} is the raw cortisol measurement, we define $z_{ij} = \log(\hat{c}_{ij})$, then use
72 linear regression on z_{ij} to define the decline as $d_{ij} = \log(A_j) - \alpha_j t_i$, and subtract this from
73 z_{ij} to obtain the normalized log cortisol in segment i for person j , $y_{ij} = \log(c_{ij}) = z_{ij} -$
74 d_{ij} . Fourier analysis was computed on $c_{ij} = \exp(y_{ij})$ using the dFFT function of python
75 v3.7.4, numpy v1.16.5.

76 Fourier analysis is a widely-used method to decompose a time-varying signal into its
77 constituent frequency components. It provides a breakdown of the signal into a sum of
78 sine waves of different frequencies. Each sine wave has an amplitude and a phase. The
79 higher the amplitude at a given frequency, the higher the contribution of that frequency to
80 the signal.

81 The number of different frequencies provided by this analysis equals half of the number
82 of time-points in the signal. For a signal with six time-points, three frequencies are
83 available: the lowest frequency corresponds to a period equal to the total duration D of
84 the 6 measurements, and the two other frequencies correspond to periods that are $1/2$
85 and $1/3$ of D . In the present case, $D=1$ year, and the frequencies correspond to sine
86 waves with periods of 1 year, 6 months and 4 months.

87 We also estimated the effect of the month of the year on cortisol measurements. For this
88 purpose, we averaged the decline-corrected c_{ij} according to the calendar month
89 corresponding to the middle of the segment, taking into account an offset of 3mm inside
90 the scalp and 8mm outside the scalp at the point of hair cutting, and a growth rate of
91 1cm/month. We then fit the resulting average, denoted $C(t)$ where t is the month of the
92 year, to a cosinor model $A \cos(\omega t + \phi)$ with $\omega = \frac{2\pi \text{ rad}}{12 \text{ month}}$. To correct for month of the year,
93 we then normalized c_{ij} by the best-fit cosinor model using the month of the year for each
94 mid-segment (see SI, S3).

95 To estimate significance, we compared our results with the Fourier analysis of a shuffled
96 control. We shuffled the segments $i = 1 \dots 6$ within each participant's normalized data c_{ij} .
97 This yielded shuffled data, s_{ij} . The shuffling keeps each participant's normalized cortisol
98 distribution but breaks temporal correlations. We then added the best-fit decline of that
99 participant, to get simulated raw log data, $z'_{ij} = \log(s_{ij}) + d_{ij}$. We then repeated the
100 analysis by fitting the decline with a new regression (which yields a slightly different
101 decline, d'_{ij} , due to the data shuffling), subtracted the decline d'_{ij} to obtain $y'_{ij} = z'_{ij} -$
102 d'_{ij} , and performed the same Fourier analysis on $\exp(y'_{ij})$. This controls for the fact that
103 the decline correction affects the long-wavelength components of the data. We repeated
104 this procedure 1,000 times in order to estimate statistical significance (See SI, S2 for
105 details).

106 We also performed a second, non-parametric analysis. We assumed that the decline of
 107 cortisol is monotonic with distance from the proximal segment. We therefore performed a
 108 rank regression on \hat{c}_{ij} versus segment number ($i = 1..6$). We then subtracted the rank
 109 regression from the rank of \hat{c}_{ij} , to obtain the rank residuals r_{ij} . Finally, we performed a
 110 Fourier analysis on r_{ij} . As a shuffled control, we shuffled r_{ij} within each participant j ,
 111 added the rank regression for that participant, rank-regressed again, and performed
 112 Fourier analysis on the residuals. The results are qualitatively similar to the parametric
 113 test and are shown in the SI, S4.

114 *HPA model*

115 We employ a recently developed model for the HPA axis, which incorporates the effects
 116 of the hormones on the total functional mass of hormone-secreting cells (Karin et al.,
 117 2020; Tendler et al., 2020). The concentrations of the hormones CRH, ACTH and cortisol
 118 are denoted x_1, x_2 and x_3 . The input to the hypothalamus, which describes the combined
 119 impact on CRH secretion due to physiological, circadian, and psychological stressors is
 120 denoted u . The total functional mass of pituitary corticotroph cells that secrete ACTH is
 121 C , and that of the adrenal cortex cells that secrete cortisol is A . The secretion of CRH due
 122 to input u is as follows:

$$123 \quad (1) \frac{dx_1}{dt} = b_1 u f(x_3) - a_1 x_1$$

124 Where b_1 is the secretion parameter of CRH, and a_1 is CRH removal rate. $f(x_3)$ describes
 125 the feedback by cortisol, due to the mineralocorticoid and glucocorticoid receptors (MR
 126 and GR, respectively) in the hypothalamus, $f(x_3) = MR(x_3) GR(x_3)$. Since the high-
 127 affinity receptor MR is usually bound by cortisol at physiological levels we use an
 128 approximation to the Michaelis–Menten binding kinetics; GR is a cooperative (n) receptor
 129 that binds cortisol with lower affinity, K_{GR} :

$$130 \quad (2) MR(x_3) = \frac{1}{x_3}$$

$$131 \quad (3) GR(x_3) = \frac{1}{1+(x_3/K_{GR})^n}$$

132 The dynamics of ACTH are as follows:

$$133 \quad (4) \frac{dx_2}{dt} = b_2 x_1 C g(x_3) - a_2 x_2$$

134 While b_2 is the secretion parameter per unit corticotroph functional mass. The parameter
 135 b_2 includes per-cell effects with signaling pathways such as CRH receptor numbers per
 136 cell, neuronal inputs and cytokine inputs that affect corticotrophs. $g(x_3)$ is the feedback
 137 from cortisol due to the GR receptors in the pituitary, $g(x_3) = GR(x_3)$.

138 The dynamics of cortisol are as follows:

$$139 \quad (5) \frac{dx_3}{dt} = b_3 x_2 A - a_3 x_3$$

140 While b_3 includes all per-cell effects on cortisol secretion rates, and a_3 is cortisol removal
141 rate. To this classical model, Karin et al. added the effects of the hormones on the total
142 functional mass $C(t)$ and $A(t)$, which are important for the present study. The mass
143 changes can be due to cell division (hyperplasia) or cell growth (hypertrophy); the precise
144 mechanism is not important for the present analysis. The main growth factor for
145 corticotrophs is CRH, so that proliferation rate is $b_c x_1$ and removal rate is a_c , resulting in
146 the following:

$$147 \quad (6) \frac{dC}{dt} = C(b_c x_1 - a_c)$$

148 Note that C occurs in both proliferation and removal terms, because differentiated
149 corticotrophs divide to produce new corticotrophs (Gulyás et al., 1991) (with additional
150 supply, not considered here, from pituitary stem cells (Andy Levy, 2007; Nakane et al.,
151 1977)). The main growth factor for cortisol-secreting cells in the adrenal cortex is ACTH
152 and therefore:

$$153 \quad (7) \frac{dA}{dt} = A(b_A x_2 - a_A)$$

154 The timescales for the change in mass are governed by the removal rates a_A and a_c ,
155 which are experimentally found to be on the scale of weeks in model organisms (A Levy,
156 2002; Nolan et al., 1998; Swann, 1940; WESTLUND et al., 1985). An analytical solution
157 of the steady state stability found a spiral fixed point with a period on the order of a year
158 (Tendler et al., 2020). The parameter values used in the present simulations are given in
159 table 1 (SI, S1). In a version of the model without cell mass dynamics, we used constant
160 $A(t) = C(t) = 1$ and omitted equations 6 and 7. We numerically solved the model using
161 python's solver, 'odeint' of scipy v1.3.1 (Virtanen et al., 2020) The input was piecewise-
162 constant u in every 2-month time period, with a value of u drawn from a lognormal
163 distribution with a mean of 1 and a standard deviation (STD) of 0.65, determined to give
164 cortisol STD similar to measurements. We simulated four years of dynamics, and took
165 the last year for analysis, in order to avoid transients due to initial conditions. We
166 simulated individual participant data by multiplying x_3 by the exponential decline fit for
167 that participant and averaging this over six consecutive 2-month periods. This generated
168 a simulated dataset with the same number of participants as the experimental data. We
169 then performed the same analysis as for the experimental cortisol measurements. To test
170 the significance of the model results, we repeated this procedure 1,000 times with new
171 simulations.

172 To complement the empirical analysis with simulations we performed an analytical
173 spectral analysis on the linearized model equations, using Bode plots (S1, S6).

174

175 S1. Table of reference parameter values, related to Figure 4

| Parameter | Value | Reference |
|-----------|----------------|-------------------------|
| b_1 | 0.17 [1/min] | (Andersen et al., 2013) |
| b_2 | 0.035 [1/min] | (Andersen et al., 2013) |
| b_3 | 0.0091 [1/min] | (Andersen et al., 2013) |
| b_P | 1/30 [1/day] | (Nolan et al., 1998) |
| b_A | 1/30 [1/day] | (Kataoka et al., 1996) |
| K_{GR} | 4 | (Karin et al., 2020) |
| n | 3 | (Andersen et al., 2013) |

176

177 S2. Statistical tests for significance of Fourier amplitudes

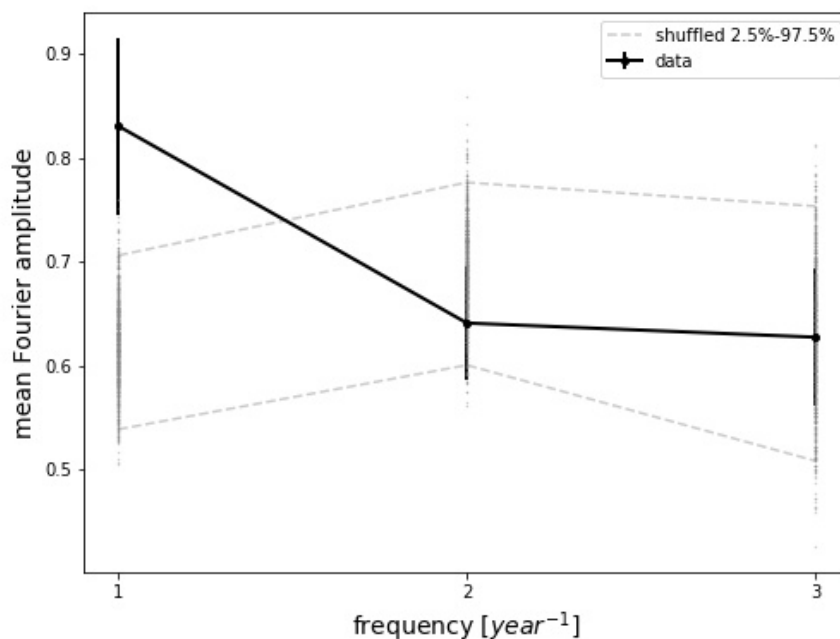
178 We tested the significance of the mean Fourier amplitude at $1[\text{year}^{-1}]$ compared to a
179 shuffled control in which the 6 time-points of each individual are shuffled. For this purpose,
180 we generated 1000 bootstrapped datasets in which we chose from the 55 participants
181 with returns. For each bootstrapped dataset we computed the mean Fourier amplitude
182 (A) at $1[\text{year}^{-1}]$. This results in a distribution $P_{bootstrap}(A)$. We then shuffled the time
183 points of each participant and generated 1000 shuffled datasets. We computed the mean
184 Fourier amplitude at $1[\text{year}^{-1}]$ for each shuffled dataset, to obtain $P_{shuffled}(A)$. We find
185 that both distributions are very close to Normal, as expected for distributions of means.
186 We then computed significance in two different ways, parametric and non-parametric.
187 The parametric test used the normality of the distribution to calculate the weighted p value

188 and effect size (Cohens d) analytically. The non-parametric calculation asked how often
189 $P_{shuffled}(A)$ exceeds $P_{bootstrap}(A)$. The effect size was calculated using Cliff's delta
190 (whose range is [-1,1]).

191 S3. Correction for seasonality shows a dominant $year^{-1}$ frequency

192 We also analyzed the data according to calendar months, using a cosinor analysis. Hair
193 cortisol showed a seasonal amplitude of $15\% \pm 3$ with a peak at May-June. We correct for
194 seasonality by dividing the decline-corrected cortisol values for each segment by the
195 cosinor model for the relevant months (Methods), and repeated the Fourier analysis.

196 Fourier analysis shows that the lowest frequency of 1 $year^{-1}$ remains the dominant
197 frequency (Figure S1). It exceeds shuffled control significantly ($p=0.01$, Cohen's $D=3.2$,
198 non-parametric $p=0.01$, Cliff's delta=0.98). We conclude that hair cortisol shows
199 variations on the scale of a year that go beyond seasonality.



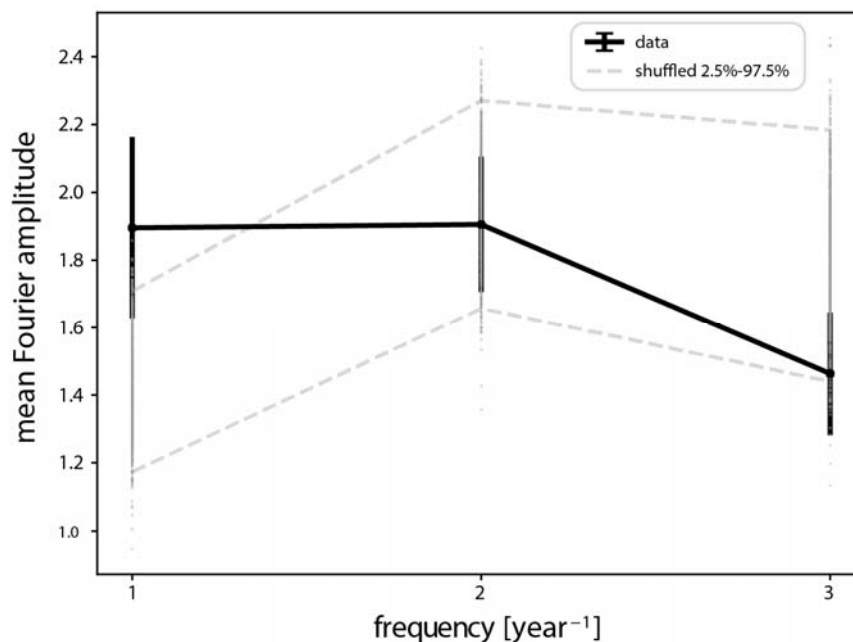
200

201 Figure S1. Hair cortisol shows fluctuations with a dominant period of 1 year, after correcting for
202 seasonality, related to Figure 3. Fourier amplitudes averaged over participants quantify the
203 contribution of each frequency component (1[$year^{-1}$], 2[$year^{-1}$] and 3[$year^{-1}$]) to the cortisol
204 signal (black dots). Error bars (SEM) were calculated by bootstrapping the participants. Shuffled
205 control is shown as gray dots (1,000 repeats), with 97.5% and 2.5% confidence intervals shown
206 in dashed gray lines.

207 The present finding of a May-June peak of hair cortisol is not consistent with most
208 previous cortisol seasonality studies that identify peak cortisol (acrophase) in winter
209 (Hadlow et al., 2018; Persson et al., 2008; Tendler et al., 2020), including a study on hair
210 cortisol on 3,507 British civil servants (Abell et al., 2016). There is one exception of a
211 large study with a peak phase in summer - a study from Netherlands on 1,768 children
212 (age 10-12) (Rosmalen et al., 2005). The reason for the discrepancy of the present peak
213 season (acrophase) with most previous studies is not clear.

214 S4. Non-parametric correction for cortisol decline shows dominant $year^{-1}$
215 frequency as well

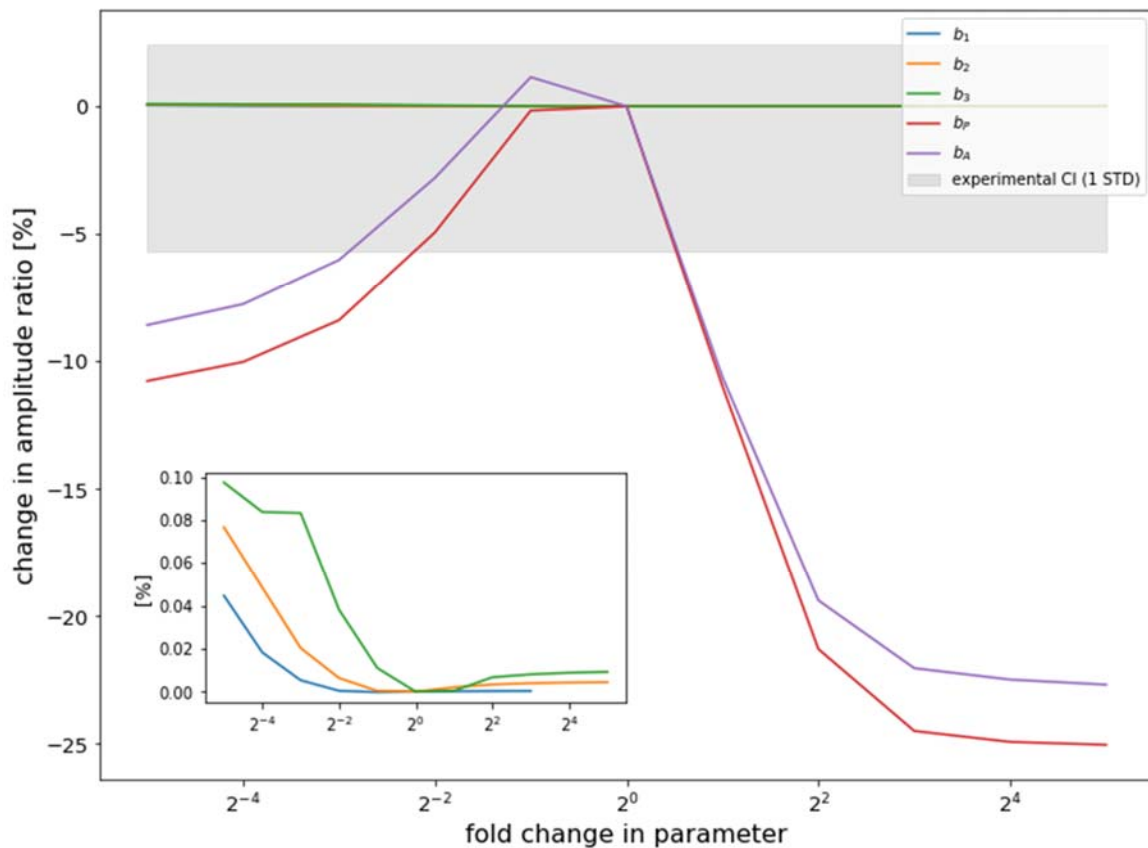
216 We made a non-parametric correction for the cortisol decline along the hair by rank
217 regression (see Methods). Despite the large loss of information due to using ranks, the
218 $1\ year^{-1}$ frequency showed a trend of being higher than shuffled control ($p=0.06$, Cohen's
219 $d=2.2$; nonparametric $p=0.06$, Cliff's $\delta=0.88$) (Figure S2). The highest mean amplitude
220 was obtained at the slowest frequency, $1\ year^{-1}$, this amplitude was about 1.3 ± 0.2 times
221 higher than the amplitude of the highest frequency, $3\ year^{-1}$.



222 Figure S2. Rank-normalized hair cortisol shows fluctuations with a dominant $year^{-1}$ frequency,
223 related to figure 3. Mean Fourier amplitudes of hair cortisol data, which was normalized by rank
224 regression (black dots with 1 STD error bars obtained by bootstrapping). Shuffled control is shown
225 as gray dots (1,000 repeats), with 97.5% and 2.5% confidence interval shown in dashed gray
226 lines.

227 S5. Sensitivity analysis of HPA model simulations

228 We tested the sensitivity of the main conclusion of the simulation analysis to the model
229 parameters. We varied each of the five model parameters around its reference value
230 (table S1) by a factor of up to $2^{10} = 1024$ -fold. For each case, we repeated the simulation
231 of Figure 4. We computed the ratio R between the 1 year^{-1} and 3 year^{-1} amplitudes.
232 Figure S3 shows the percent change in R as a function of the fold-change in each
233 parameter. The slow-timescale parameters for the tissue turnover processes, b_A and b_P ,
234 match the observed ratio within its experimental error (gray region) over an approximately
235 8-fold range around their reference values. The fast timescale parameters, that describe
236 hormone production and removal, have minor effects on R across the entire 1024-fold
237 range (inset). We conclude that the dominance of the 1 year^{-1} frequency is insensitive
238 to the model parameters.



239 Figure S3. Sensitivity analysis of HPA model with mass dynamics suggests that the dominance
240 of the low frequency is insensitive to all model parameter, related to Figure 4 and Table S1. Each
241 of the five model parameters was varied around its reference range by a range of $2^{10} = 1024$. For
242 each case, the simulation of Figure 4 was repeated, and the ratio between the 1 year^{-1} and
243 3 year^{-1} amplitudes was computed. The plot shows the percent change in the ratio as a function
244 of the fold change in each parameter. The slow-timescale parameters for the tissue turnover

245 processes, b_A and b_P , match the observe ratio within its experimental error (gray region) for an
246 approximately 8-fold range. The fast timescale parameters of hormone production and removal
247 have minor effects on the ratio across the entire range (inset).

248 S6. Frequency response of the linearized HPA model

249 In order to put the findings in perspective, and to add analytical understanding, we
250 calculate here the frequency response of the linearized HPA model. The frequency
251 response allows one to calculate the magnitude and the phase of the system's output as
252 a function of frequency, for a given input. We analyze the system around its steady state.
253 Although in reality the simulations are not strictly in the linear range, the linear
254 approximation can be used to gain intuition. We thus assume $x_3 \ll K_{GR}$, therefore the
255 GR is not activated and we can set $GR(x) = 1$. Substituting this in the model equations
256 (1)-(7) (Methods). We used dimensionless variables for the hormones and glands. We do
257 so by normalizing the steady-state of all variables to be 1 for an input $u = 1$. Scaling the
258 variables gives:

$$259 \quad \frac{dx_1}{dt} = b_1 \left(\frac{u}{x_3} - x_1 \right)$$

$$260 \quad \frac{dx_2}{dt} = b_2 (Cx_1 - x_2)$$

$$261 \quad \frac{dx_3}{dt} = b_3 (Ax_2 - x_3)$$

$$262 \quad \frac{dC}{dt} = b_C C (x_1 - 1)$$

$$263 \quad \frac{dA}{dt} = b_A A (x_2 - 1)$$

264 The linearization of these equations around their steady state and using a Laplace
265 transform gives:

$$266 \quad sX_1(s) = b_1 (U(s) - X_1(s) - X_3(s))$$

$$267 \quad sX_2(s) = b_2 (X_1(s) - X_2(s) + C(s))$$

$$268 \quad sX_3(s) = b_3 (X_2(s) - X_3(s) + A(s))$$

$$269 \quad sC(s) = b_C X_1(s)$$

$$270 \quad sA(s) = b_A X_2(s)$$

271 The capital letters denote the Laplace transform of each variable. Solving these equations
272 we get:

$$273 \quad H_1(s) = \frac{X_1(s)}{U(s)} = \frac{b_1(b_2 + s)(b_3 + s)s^2}{D(s)}$$

$$274 \quad H_2(s) = \frac{X_2(s)}{U(s)} = \frac{b_1b_2(b_3 + s)(b_C + s)s}{D(s)}$$

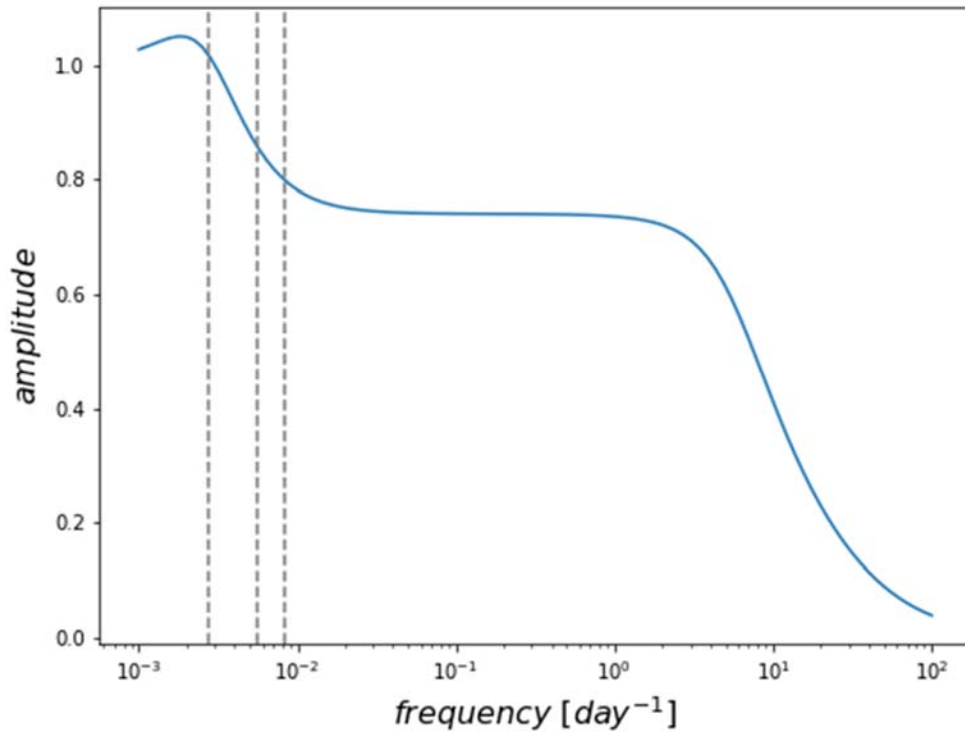
$$275 \quad H_3(s) = \frac{X_3(s)}{U(s)} = \frac{b_1b_2b_3(b_C + s)(b_A + s)}{D(s)}$$

$$276 \quad H_C(s) = \frac{C(s)}{U(s)} = \frac{b_1b_C(b_2 + s)(b_3 + s)s}{D(s)}$$

$$277 \quad H_A(s) = \frac{A(s)}{U(s)} = \frac{b_1b_2b_A(b_3 + s)(b_C + s)}{D(s)}$$

278 Where $D(s) = s^5 + (b_1 + b_2 + b_3)s^4 + (b_1b_2 + b_1b_3 + b_2b_3)s^3 + 2b_1b_2b_3s^2 + b_1b_2b_3(b_A +$
279 $b_C)s + b_1b_2b_3b_Ab_C$

280 $H_x(s)$ are the transfer functions of each variable. By substituting $s = j\omega$ ($j = \sqrt{-1}$), we
281 obtain the frequency response of the system. The amplitude of each variable as function
282 of frequency is obtained by calculating the magnitude of the transfer function, $A_x =$
283 $|H_x(j\omega)|$. Using the parameters listed in table S1 we plot the cortisol frequency response
284 (Figure S4). Note that a white noise input corresponds to input with constant amplitude at
285 each frequency. Thus, the frequency response curve corresponds to the Fourier
286 amplitudes expected for a white noise input. At very high frequencies corresponding to
287 periods of days or hours, the response decays. At frequencies of around 1 year^{-1} the
288 frequency response shows the qualitative trend observed in the present study: the
289 1 year^{-1} frequency has higher amplitude than the 2 year^{-1} and 3 year^{-1} frequencies as
290 found in the results section. Note that frequencies slower than 1 year^{-1} are also predicted
291 to occur. Observing such variations with a period longer than a year require a longer
292 longitudinal study.



293

294 Figure S4. Analytical linearized frequency response for cortisol shows dominant $year^{-1}$
 295 frequency, related to Figure 3. Cortisol amplitude as function of the stressor input frequency in
 296 the HPA model with mass dynamics. Vertical dashed lines correspond to the frequencies in the
 297 hair cortisol experiment - 1,2 and 3 $year^{-1}$.

298 S7. Analysis of the gland turnover times

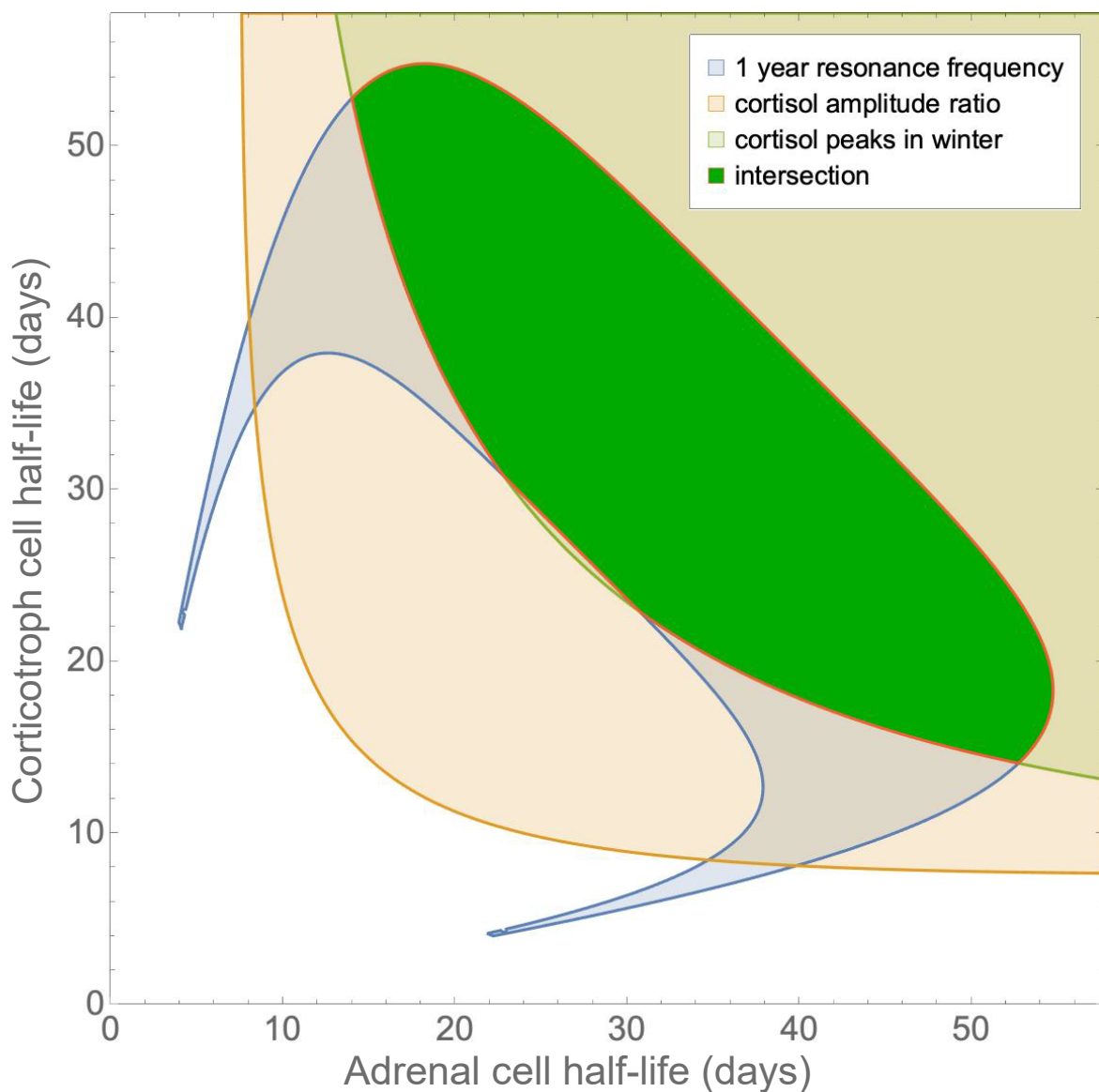
299 Combining theoretical hypotheses and experimental evidence, we construct different
 300 independent constraints on the relationships between the parameters of the gland
 301 turnover rates (a_C and a_A). Each constraint is projected onto the parameter space and is
 302 satisfied in some region of this space (Figure S5). The intersection (if it exists) between
 303 these different regions provides a range of consistent parameter values.

304 Using the linearized frequency response of the HPA system (SI, S6) and the experimental
 305 results of this study, one can constrain the turnover parameters to fulfill a condition on the
 306 ratio between the cortisol amplitudes $|H_3|$ at the slowest frequency ($1 year^{-1}$), to the
 307 fastest ($3 year^{-1}$). The experimentally observed ratio is in the range

308
$$1.3 < \frac{|H_3(w = 1 year^{-1})|}{|H_3(w = 3 year^{-1})|} < 1.65$$

309 We added this constraint to the ones discovered in a previous study (Tendler et al., 2020)
310 on seasonal entrainment of the hormone circuit: 1) A resonance frequency of
311 approximately 1 year (range 9-13 months) for the gland-mass negative feedback circuit;
312 2) Experimental observation that cortisol blood and urine tests peak at late winter.

313 These constraints are independent, and hence a-priori they do not have to converge in a
314 specific intersection region. The existence of a region (green region) provides a consistent
315 parameter range. Reassuringly, this range is consistent with gland turnover
316 measurements in model organisms (GERTZ et al., 1987; Kataoka et al., 1996; Nolan et
317 al., 1998; WESTLUND et al., 1985).



319 Figure S5. Constraint analysis for gland turnover parameters suggests a range consistent
320 between several independent measurements, related to Figure 4 and Table S1. Each region
321 corresponds to parameter values that satisfy a certain constraint. (i) ratio between 1 year^{-1} and
322 3 year^{-1} frequencies in response to white noise in the present experimental range (orange
323 region). (ii) cortisol peak in winter for a seasonal input as measured and calculated in Tendler et
324 al. (light green) (iii) resonance frequency of the linearized model in the range of 9-13 months (blue
325 region). Intersection: dark green region.

326

327